

# Low threshold and broad tunability of an organic optical parametric oscillator

D. Josse, S. Khodja, J. Badan, I. D. W. Samuel, and J. Zyss

France Telecom, CNET-PARIS B, Laboratoire de Bagneux, Département d'Electronique Quantique et Moléculaire, 196 Avenue Henri Ravéra, BP107, 92225 Bagneux Cedex, France

(Received 13 January 1994; accepted for publication 12 April 1994)

Optical parametric oscillation in the molecular organic crystal NPP [*N*-(4-nitrophenyl)-*L*-prolinol] is reported at a pumping wavelength of 670 nm with pulse duration of 60 ns, and improved performance over the earlier demonstration at 592.7 nm pump wavelength (pulse duration 1 ns). The pumping scheme is simplified, the oscillation threshold substantially decreased by more than an order of magnitude to 0.5 MW/cm<sup>2</sup>, with the benefit of an increasingly wavelength noncritical configuration as the pump wavelength is shifted towards the infrared.

The interest in optical parametric oscillators (OPO)<sup>1</sup> initially spurred by the diversity of applications ranging from spectroscopy, environmental monitoring, and telecommunications, has been recently revived<sup>2,3</sup> by technological advances pertaining to laser pumping sources and nonlinear crystals. The former are more stable and flexible in terms of pulse duration and emission wavelength while the diversity, efficiency, and optical quality of nonlinear materials has benefited from two decades of research in the realm of inorganic crystals such as  $\beta$ -BaB<sub>2</sub>O<sub>4</sub> (BBO) and LiB<sub>3</sub>O<sub>5</sub> (LBO)<sup>2,3</sup> as well as organic crystals.<sup>4</sup> Furthermore, new developments based on quantum phenomena related to the specific statistical properties of the coherent emission of pairs of photons have contributed to this upsurge of activity.

Among currently developed nonlinear crystals, organic molecular crystals stand out in view of their high nonlinearity, and high damage threshold in the pulsed regime. Adequate spectral tailoring is achieved in the case of the paranitroaniline family, for pumping in the visible or near infrared with optical emission in the wavelength range encompassing optical fiber transmission windows.

Whereas the first demonstration of an organic crystal-based OPO made use of urea,<sup>5</sup> its displaced transparency towards the near ultraviolet (UV) and ensuing low nonlinearity, absence of phase matching in the near infrared (IR), together with practical problems linked to hygroscopy did not qualify urea for practical applications in the near IR. Among members of the more adequately tailored paranitroaniline family, NPP [*N*-(4-nitrophenyl)-*L*-prolinol] stands out in view of its high nonlinearity ( $d_{\text{eff}}=57$  pm/V at 1340 nm),<sup>6</sup> its suitability for parametric amplification in the femtosecond regime<sup>7,8</sup> and more recently, the first demonstration of near IR optical parametric oscillation in an organic crystal at a pumping wavelength of 592.7 nm and pulse duration of 1 ns.<sup>9-11</sup> These remarkable properties result from the "optimized" arrangement<sup>12</sup> of the chromophore units in the monoclinic unit cell. However, the initial pumping system consisting of two synchronized, frequency mixed Nd<sup>3+</sup>:YAG lasers, respectively, at 1340 and 1064 nm was rather involved, leaving room for simplification and eventual shifting of the pumping wavelength towards the red so as to achieve a better conversion yield at telecommunication wavelengths while decreasing the pump absorption as reported hereafter.

As compared to the earlier scheme at 592.7 nm, we report here a simpler pumping source at 670 nm: in initial experiments<sup>9</sup> the 592.7 nm pump was obtained by type II noncollinear sum-frequency generation of 1064 and 1338 nm Nd<sup>3+</sup>:YAG lasers in KTP giving light pulses of 1 ns duration with an energy of 0.41 mJ at a repetition rate of 5 Hz. The (gaussian) pump beam radius,  $\omega_0$ , was 0.5 mm. In current experiments, the 670 nm pump is generated by frequency doubling a 1340 nm *Q*-switched Nd<sup>3+</sup>:YAG laser in a crystal of KTP, producing a maximum output of 2 mJ at 670 nm, with pulses of 60 ns duration at a repetition rate of 5 Hz. The radius of the pump beam,  $\omega_0$ , on the NPP crystal was measured by an optical multichannel analyzer (OMA) to be 1 mm. The OPO cavity is resonant at both signal and idler wavelengths in order to reduce the oscillation threshold.<sup>13</sup> The input mirror is curved with a radius of 2000 mm and a transmission at the pump wavelength greater than 96%. The output mirror is planar with a reflectivity at 1.3  $\mu\text{m}$  of 85%, thus leading to a semiconfocal design of the cavity.

Rather than cutting the crystal at normal incidence with respect to the phase-matching direction, it was preferred to benefit from the availability of the as-grown (*XY*) principal dielectric plane coinciding with the (101) cleavage plane, with the type I phase-matching direction in the (*XZ*) plane at the fundamental wavelength  $\lambda=1.34$   $\mu\text{m}$  accessible at an angle  $\theta=32.69^\circ$  with respect to the normal to the surface. However, as a result of the reflection losses in such a configuration, only a part of the incident energy is useful, thus increasing the risk of damage at the entrance face of the crystal. Therefore, in order to reduce the angle of incidence, the NPP crystal was immersed in an index-matching liquid filled cell with refractive index  $n=1.303$ , thus reducing the angle of incidence in the crystal, down to an internal value of  $\theta'=24^\circ$ . The minimum cavity length  $L$ , as limited by the physical size of the liquid cell, is 25 mm. The NPP crystal dimensions are 5 $\times$ 2 $\times$ 3 mm<sup>3</sup> with 3 mm along the *Z* axis. As a result of refraction in the crystal at shorter signal or longer idler wavelengths, the three wave vectors of the pump, signal, and idler beams are not exactly collinear. Tuning of the OPO is obtained in a type I phase-matching (PM) configuration by rotating the crystal about its *Y* axis parallel to the pump polarization direction.

For the pump wavelength at 592.7 nm, the degenerate

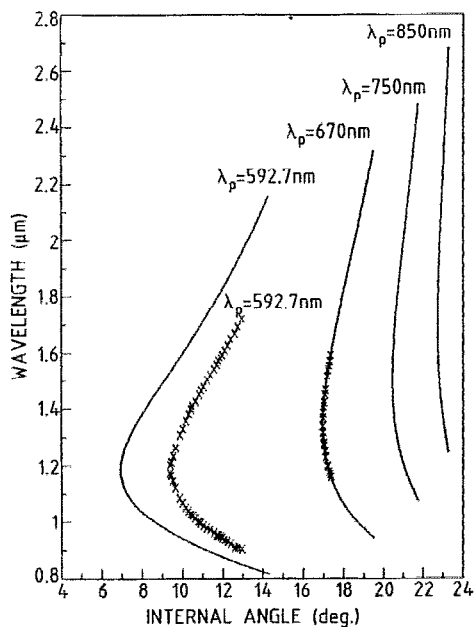


FIG. 1. Angle tuning curves of the NPP-based OPO: the points are experimental data and the solid curves are calculated from the Sellmeier equations (Ref. 6). The phase matching configuration tends to be  $\theta$  noncritical at  $\lambda_p=592.7$  nm pump wavelength.  $\lambda$ -noncritical phase-matching configurations prevail for a pump wavelength shifted towards the infrared. At 670 nm the range of experimental data points is limited by the reflectivity of the cavity mirrors.

PM direction of the OPO is close to the  $Z$  axis making it less angle critical and thereby limiting the walk off of the signal and idler beams, with a tuning range extending from 0.9 to 1.7  $\mu\text{m}$  (see Fig. 1<sup>14</sup>).

For the longer pumping wavelength (670 nm), the PM direction is far from that of the  $Z$  axis, leading to a walk-off angle of the order of  $11.4^\circ$  at the degenerate PM configuration, so that the interaction length for which the conversion efficiency remains significant is shorter than the physical

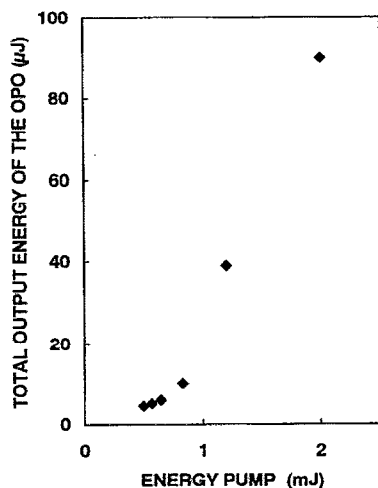


FIG. 2. Total output energy of the NPP-based OPO near degeneracy as a function of the pump energy at 670 nm. The length of the crystal along the propagation coordinate is 3 mm, and the cavity length is 25 mm.

TABLE I. Comparison of the performance of the NPP-based OPO in the two pumping configurations.

	First OPO	Present OPO
Pump wavelength	592.7 nm	670 nm
Pump duration (FWHM)	1 ns	60 ns
Repetition rate	5 Hz	5 Hz
Crystal thickness	1.9 mm	3 mm
OPO cavity length	12 mm	25 mm
Pump peak intensity	71 MW/cm <sup>2</sup>	2.3 MW/cm <sup>2</sup>
Pump beam radius $\omega_0$	0.5 mm	1 mm
Energy per pump pulse	0.41 mJ	2 mJ
Emitted maximal energy (signal and idler)	20 $\mu\text{J}$	90 $\mu\text{J}$
Yield	5%	4.5%
Threshold intensity	11 MW/cm <sup>2</sup>	0.47 MW/cm <sup>2</sup>

length of the crystal. The interaction length tends to decrease away from degeneracy as a result of the increased walk off. The measured spectral tuning range is shown in Fig. 1. The range of experimentally available emitted wavelengths is presently limited by the reflectivity of the cavity mirrors which is high only in the vicinity of degeneracy.

Figure 1 also shows the quasivertical outlook of the tuning curves at longer pump wavelength due to the strong dispersion of the refractive indices. In this case the PM configuration is more angle critical, which enables the full tuning range to be covered by a very small rotation ( $1^\circ$ ) of the crystal about the  $Y$  axis whereas the spectral acceptance is very large (i.e.,  $\lambda$  noncritical). This last feature is of great interest for short pulse applications where group velocity dispersion needs to be minimized.<sup>8</sup> It is, however, largely responsible for the broad bandwidth of the OPO output measured to be of the order of 40 nm at degeneracy, although other factors, such as the linewidth of the pump laser, the divergence of the pumping beam, and the cavity parameters also contribute.

For the 670 nm pump radiation the oscillation threshold intensity is less than 0.5 MW/cm<sup>2</sup> close to degeneracy at a minimal cavity length of 25 mm. This threshold intensity is considerably smaller than the value of 11 MW/cm<sup>2</sup> observed at a pump wavelength of 592.7 nm. The reduction by a factor of more than 20 mainly originates from the improved transparency of the crystal at 670 nm, which permits the use of longer pump pulses and hence benefit from an increased number of round trips within the OPO cavity. Note that no correction has been made for reflection of the 670 nm pump beam. The threshold intensity compares very favorably with the 10 MW/cm<sup>2</sup> typical of pulsed OPOs based on inorganic crystals.<sup>15</sup>

The total energy output of the OPO for both signal and idler near degeneracy increases with input pump energy as shown in Fig. 2. For longer pump wavelengths, the NPP crystal becomes more transparent,<sup>10</sup> thus further increasing the damage threshold and opening the way to longer pump pulse duration. We obtained a yield of approximately 5% in both configurations, but the energy per pulse for the pump at 670 nm rises to 90  $\mu\text{J}$ , as compared to 20  $\mu\text{J}$  for the pump at 592.7 nm. The performance of the OPO in the two pumping

configurations at 592.7 and 670 nm is summarized and compared in Table I.

In conclusion, we have demonstrated the successful operation of a NPP-based OPO pumped at 670 nm, in a simplified and hence applicable configuration. Although the effective nonlinear coefficient is smaller than in the earlier 592.7 nm configuration, the oscillation threshold is reduced by a factor of more than 20 down to a remarkably low value of  $0.5 \text{ MW/cm}^2$  as a result of the increased transparency at 670 nm. The tendency towards  $\lambda$ -noncritical operation as the pump wavelength is further shifted to the infrared opens up interesting possibilities, in particular in the realm of subpicosecond operation.

This work was partly supported by a U.S. Navy Grant for "Highly Efficient Optically Nonlinear Materials."

<sup>1</sup>R. L. Byer, in *Optical Parametric Oscillators*, edited by H. Rabin and C. L. Tang (Academic, New York, 1975), Vol. 1, p. 557.

<sup>2</sup>R. L. Byer and A. Piskarskas, *J. Opt. Soc. Am. B* **9**, 1655 (1993).

<sup>3</sup>R. L. Byer and A. Piskarskas, *J. Opt. Soc. Am. B* **9**, 2146 (1993).

<sup>4</sup>See, for example, *Molecular Nonlinear Optics: Materials, Physics and Devices*, edited by J. Zyss (Academic, Boston, 1993).

<sup>5</sup>W. R. Donaldson and C. L. Tang, *Appl. Phys. Lett.* **44**, 25 (1983).

<sup>6</sup>I. Ledoux, C. Lepers, A. Périgaud, J. Badan, and L. Zyss, *Opt. Commun.* **80**, 149 (1990).

<sup>7</sup>I. Ledoux, J. Zyss, A. Migus, J. Etchipare, G. Grillon, and A. Antonetti, *Appl. Phys. Lett.* **48**, 1564 (1986).

<sup>8</sup>I. Ledoux, J. Zyss, A. Migus, D. Hulin, and A. Antonetti, *J. Appl. Phys.* **64**, 3309 (1988).

<sup>9</sup>D. Josse, S. X. Dou, J. Zyss, P. Andreazza, and A. Périgaud, *Appl. Phys. Lett.* **61**, 121 (1992).

<sup>10</sup>S. X. Dou, D. Josse, and J. Zyss, *J. Opt. Soc. Am.* **10**, 1708 (1993).

<sup>11</sup>J. Zyss, *J. Phys. D: Appl. Phys.* **26**, B198 (1993).

<sup>12</sup>J. Zyss, J. F. Nicoud, and M. Coquillay, *J. Chem. Phys.* **81**, 4160 (1984).

<sup>13</sup>F. G. Colville, A. J. Henderson, M. J. Padgett, J. Zhang, and M. H. Dunn, *Opt. Lett.* **18**, 205 (1993).

<sup>14</sup>The difference between the Sellmeier calculation and the experimental data at 592.7 nm is mainly due to the wavelength dispersion of the orientation of the non-symmetry frozen Z axis. The axis rotation is more significant close to resonance, e.g., at 592.7 nm, than at 670 nm, hence better agreement in the latter case. Related considerations are developed in P. Andreazza, D. Josse, F. Lefaucheux, M. C. Robert, and J. Zyss, *Phys. Rev. B* **45**, 7640 (1992).

<sup>15</sup>Y. Wang, Z. Xu, D. Deng, W. Zheng, X. Liu, B. Wu, and C. Chen, *Appl. Phys. Lett.* **58**, 1461 (1991).